

AD-A038 822

IOWA UNIV IOWA CITY DEPT OF PHYSICS AND ASTRONOMY

F/6 3/2

STEREOSCOPIC DIRECTION FINDING ANALYSIS OF A TYPE III SOLAR RAD--ETC(U)

APR 77 D A GURNETT, M M BAUMBACK

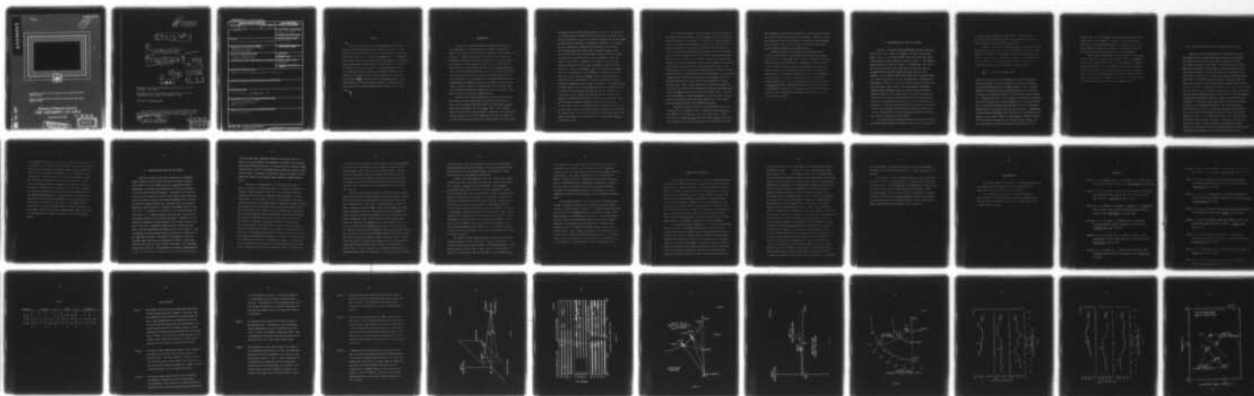
N00014-76-C-0016

UNCLASSIFIED

U. OF IOWA-77-13

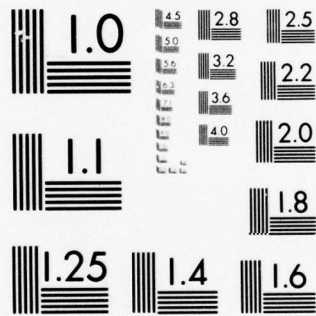
NL

| OF |  
AD  
A038822



END

DATE  
FILMED  
5-77



MICROCOPY RESOLUTION TEST CHART  
NATIONAL BUREAU OF STANDARDS-1963-A

12  
B.S.

AD A 038822



"Reproduction in whole or in part is permitted for any purpose of the United States Government.

Research was supported in part by the Office of Naval Research under Contract N00014-76-C-0016."

Department of Physics and Astronomy  
**THE UNIVERSITY OF IOWA**

Iowa City, Iowa 52242

**DISTRIBUTION STATEMENT A**  
Approved for public release  
Distribution Unlimited

97 **DDC**  
**RECEIVED**  
APR 28 1971  
**RECEIVED**

DDC FILE COPY

12  
14 U. of Iowa 77-13

9 Progress / Rept.

6  
Stereoscopic Direction Finding Analysis  
of a Type III Solar Radio Burst:  
Evidence for Emission at 2f<sub>p</sub>  
by  
D. A. Gurnett\*, M. M. Baumbach\*,  
and H. Rosenbauer

← verbalized

ACCE	White Section	<input checked="" type="checkbox"/>
PTIS	Buff Section	<input type="checkbox"/>
DOC		<input type="checkbox"/>
UNANNOUNCED		
IDENTIFICATION		
BY		
DISTRIBUTION/AVAILABILITY CODES		
Dist.	Attn.	and/or SPECIAL
A		

12 47p.

11  
Apr 28 1977

\*Department of Physics and Astronomy, the University of Iowa,  
Iowa City, Iowa 52242

\*Max-Planck-Institut für Physik und Astrophysik, Institut für  
extraterrestrische Physik, 8046 Garching, Germany

Submitted to J. Geophys. Res.

The research at the University of Iowa was supported in part  
by NASA under Contracts NAS5-11431, NAS1-13129 and NAS5-11279, and  
Grant NGL-16-001-043 and by the Office of Naval Research under  
Contract N00014-76-C-0016,

15  
NAS5-11431

DDC  
APR 28 1977

188460

UNCLASSIFIED

SECURITY CLASSIFICATION OF THIS PAGE (When Data Entered)

REPORT DOCUMENTATION PAGE		READ INSTRUCTIONS BEFORE COMPLETING FORM
1. REPORT NUMBER U. of Iowa 77-13 ✓	2. GOVT ACCESSION NO.	3. RECIPIENT'S CATALOG NUMBER
4. TITLE (and Subtitle)		5. TYPE OF REPORT & PERIOD COVERED Progress, April 1977
		6. PERFORMING ORG. REPORT NUMBER
7. AUTHOR(s) D. A. Gurnett, M. M. Baumbach and H. Rosenbauer		8. CONTRACT OR GRANT NUMBER(s) N00014-76-C-0016
9. PERFORMING ORGANIZATION NAME AND ADDRESS Department of Physics and Astronomy The University of Iowa Iowa City, IA 52242		10. PROGRAM ELEMENT, PROJECT, TASK AREA & WORK UNIT NUMBERS
11. CONTROLLING OFFICE NAME AND ADDRESS Office of Naval Research Arlington, Virginia 22217		12. REPORT DATE April 1977
		13. NUMBER OF PAGES 38
14. MONITORING AGENCY NAME & ADDRESS (if different from Controlling Office)		15. SECURITY CLASS. (of this report) UNCLASSIFIED
		15a. DECLASSIFICATION/DOWNGRADING SCHEDULE
16. DISTRIBUTION STATEMENT (of this Report)  Approved for public release; distribution is unlimited.		
17. DISTRIBUTION STATEMENT (of the abstract entered in Block 20, if different from Report)		
18. SUPPLEMENTARY NOTES  To be published in <u>J. Geophys. Res.</u> , 1977.		
19. KEY WORDS (Continue on reverse side if necessary and identify by block number)  Stereoscopic Direction Finding Type III Solar Radio Burst Radio Emission		
20. ABSTRACT (Continue on reverse side if necessary and identify by block number)  [See Page following]		

## ABSTRACT

↙ Stereoscopic direction finding measurements from the IMP 8, Hawkeye 1 and Helios 2 spacecraft over baseline distances of a substantial fraction of an A.U. are used to directly determine the three-dimensional trajectory of a type III solar radio burst. By comparing the observed source positions with the direct in situ solar wind plasma density measurements obtained by Helios 1 and 2 near the sun the relationship of the emission frequency to the local plasma frequency can be determined directly without any modeling assumptions. These comparisons show that the type III radio emission occurs near the second harmonic ~~/2f<sub>p</sub>~~ of the local electron plasma frequency. Other characteristics of the type III radio emission, such as the source size, which can be obtained from this type of analysis are also discussed.

↗

## I. INTRODUCTION

Stereoscopic direction finding measurements from the Helios 1 and 2 spacecraft, in orbit around the sun, and from the IMP 8 and Hawkeye 1 satellites, in orbit around the earth, are used to track a low frequency ( $< 1$  MHz) type-III solar radio burst in three dimensions, independent of modeling assumptions concerning the emission frequency as a function of radial distance from the sun. By combining these radio direction finding measurements with direct in situ measurements of the solar wind plasma density near the sun, the relationship between the emission frequency and the local electron plasma frequency,  $f_p^-$ , can be determined. This relationship is of fundamental importance for understanding the mechanism by which type-III radio emissions are generated. As will be shown by a detailed analysis of a type-III radio burst using this technique the dominant emission occurs at the second harmonic,  $2f_p^-$ , of the electron plasma frequency.

Type III radio bursts are produced by electrons ejected from a solar flare and are characterized by an emission frequency which decreases with increasing time [Wild, 1950; Lin, 1970; Alvarez et al., 1972; Frank and Gurnett, 1972; Lin et al., 1973]. The decreasing emission frequency with increasing time is attributed to the decreasing electron density, hence electron plasma frequency,  $f_p^-$ , encountered by the solar flare electrons as they move outward through the solar corona.

According to current theories the generation of type III radio emissions is a two-step process in which (1) electrostatic electron plasma oscillations are produced at  $f_p^-$  by a two-stream instability and (2) the plasma oscillations are converted to electromagnetic radiation by non-linear wave-wave interactions [Ginzburg and Zheleznyakov, 1958; Sturrock, 1961; Tidman et al., 1966, Smith, 1975; Papadopoulos et al., 1974]. The occurrence of intense electron plasma oscillations in association with type III solar radio bursts has been confirmed by Gurnett and Anderson [1976, 1977]. Depending on the details of the non-linear interaction the radio emission can be generated at either the fundamental,  $f_p^-$ , or the second harmonic,  $2f_p^-$ , of the local electron plasma frequency. The radiation at the fundamental is caused by the interaction of electron plasma oscillations with ion sound waves and the radiation at the second harmonic is caused by interactions between oppositely propagating electron plasma oscillations. At high frequencies,  $\geq 10$  MHz, radiation at both the fundamental and the second harmonic can be detected in the frequency-time spectrums of type III radio bursts [Wild et al., 1954]. However, at lower frequencies,  $\leq 10$  MHz, the dispersion characteristics of type III bursts are such that the fundamental and second harmonic components cannot be easily resolved. Current evidence based on statistical analyses of average burst properties and various modeling techniques indicates that for low frequencies the dominant emission is at the second harmonic [Fainberg et al., 1972; Haddock and Alvarez, 1973; Fainberg and Stone, 1974; Alvarez et al., 1975; Kaiser, 1975].

The first measurements of the trajectory of a low frequency type III radio burst were obtained by Fainberg et al. [1972] using direction finding measurements from the IMP 6 spacecraft. The technique used consists of analyzing the spin modulation caused by the rotating antenna pattern to determine the direction of arrival of the radio emission. For an electric dipole antenna oriented perpendicular to the spacecraft spin axis the spin modulation gives the direction of arrival projected onto the plane of rotation of the antenna. Since only one angle of the direction of arrival is provided by this technique additional assumptions must be made to determine a unique trajectory for the type III burst. Using a model for the average emission frequency as a function of radial distance from the sun derived from a statistical analysis of the dispersion characteristics of many type III bursts, Fainberg et al. were able to determine the projection of the type III bursts trajectory onto the ecliptic plane. Their results showed that the trajectories projected onto the ecliptic plane closely matching the expected Archimedean spiral form of the magnetic field in the solar wind [Parker, 1958]. Type III bursts are expected to follow the magnetic field lines because the energetic electrons which produce the radio emission are closely guided along the magnetic field in the interplanetary medium.

Since the spin axis of IMP 6 is oriented perpendicular to the ecliptic plane no information could be obtained by Fainberg et al. on the component of the trajectory out of the ecliptic plane. Later measurements by Baumbach et al. [1976] and Alvarez et al. [1976] using two spacecraft with nearly orthogonal spin axis orientations provided

two coordinates of the direction of arrival so that the source position out of the ecliptic plane could also be determined. However, even with this technique it was still necessary to determine the radial distance of the source from the sun on the basis of an assumed model for the average emission frequency versus radial distance.

Although trajectories obtained using the average emission frequency model have the correct qualitative characteristics, large errors can occur in individual events because of deviations of the solar wind density from the average model. Furthermore, comparisons of the emission frequency with the local electron plasma frequency cannot be performed with high accuracy because of the implicit requirement to assume a model for the emission frequency as a function of radial distance from the sun. As will be shown, the stereoscopic direction finding analyses used in this study completely eliminate the need for any a priori assumption regarding the emission frequency as a function of radial distance from the sun, thereby providing a direct method for determining the relationship of the emission frequency to the local electron plasma frequency.

## II. INSTRUMENTATION AND METHOD OF ANALYSIS

Radio wave and plasma density measurements from five spacecraft, Helios 1 and 2, IMP 7 and 8, and Hawkeye 1, are used in this study. Helios 1 and 2 are in eccentric solar orbits near the ecliptic plane with perihelion radial distances of 0.309 and 0.290 A. U. and aphelion radial distances of 0.985 and 0.983 A. U., respectively. IMP 7 and 8 are in low eccentricity earth orbits near the equatorial plane at geocentric radial distances ranging from about 23.1 to 46.3  $R_e$ . Hawkeye 1 is in a highly eccentric earth orbit with the apogee located at a radial distance of 20.5  $R_e$  over the north pole. The radio wave measurements presented are from very similar University of Iowa plasma wave instruments on the Helios 2, IMP 8 and Hawkeye 1 spacecraft. Although these instruments differ in certain details the essential features relevant to this study are that (1) the radio emissions are detected by an electric dipole antenna whose axis is oriented perpendicular to the spacecraft spin axis and (2) the wave intensities are analyzed by a series of narrow-band filter channels which are the same for all three spacecraft (four channels per decade and bandwidths of  $\pm 7.5\%$ ). Further details of these experiments are given by Kurth et al. [1975] and Gurnett and Anderson [1977].

The plasma density measurements used in this study are from the Max-Planck-Institut plasma experiments on Helios 1 and 2 and from the

Los Alamos plasma experiments on IMP 7 and 8. Details of these instruments and the procedures used in the data analysis are given by Schwenn et al. [1975] and Asbridge et al. [1976].

In order to interpret the three-dimensional radio direction finding measurements presented in this study it is important to briefly review the method of analysis and the geometry used for determining the source position. The direction of arrival of a radio wave is determined by a least square fit of the measured electric field intensities to a theoretical equation for a spin modulation envelope given by

$$\left(\frac{E}{E_0}\right)^2 = \left(1 - \frac{m}{2}\right) - \frac{m}{2} \cos [2(\varphi_A - \alpha)] ,$$

where  $E$  is the measured field strength and  $\varphi_A$  is the corresponding orientation angle of the electric antenna in the plane of rotation. The parameters determined by the fitting procedure, which is usually applied to a sequence of about 10 minutes of data, are the direction of arrival  $\alpha$ , the modulation factor  $m$ , and the electric field strength  $E_0$ . As mentioned earlier it is only possible to determine the direction of arrival projected onto a plane perpendicular to the spacecraft spin axis. The spin axis directions of both Helios and IMP 8 are oriented perpendicular to the ecliptic plane as shown in Figure 1. Simultaneous direction finding measurements from Helios and IMP 8 therefore give the angles  $\alpha_1$  and  $\alpha_2$  shown in Figure 1, which uniquely determines the position of the source projected onto the ecliptic plane. Hawkeye 1 on the other hand has its spin axis oriented nearly parallel to the

ecliptic plane. From the Hawkeye 1 the angle of arrival  $\beta_1$  above the ecliptic plane can be computed. As shown in Figure 1 these three angles,  $\alpha_1$ ,  $\alpha_2$ , and  $\beta_1$  completely specify the position of the source. By performing this analysis as a function of frequency the three-dimensional trajectory of the type III burst can be determined.

Several geometric constraints limit the number of type-III radio bursts to which this technique can be applied. Since the propagation of radio waves emitted near the sun is strongly limited by refraction effects, Helios must be on the earthward side of the sun to detect a type-III burst which can be detected at the earth. Also, large errors occur in the position determination if the baseline distance between Helios and the earth is too small ( $\leq 0.2$  A. U.) or if the angle between the baseline and the source position is too small ( $\leq 20^\circ$ ).

## III. ANALYSIS OF THE TYPE III RADIO BURST ON MARCH 23, 1976

Because of the low occurrence of solar flare activity during solar minimum and the previously mentioned geometrical constraints the number of type III radio bursts which are currently available for a detailed analysis is very small. One event for which all of the spacecraft involved were in particularly favorable positions for analysis occurred on March 23, 1976. The onset time of this event is at about 0843 UT as determined by ground high frequency radio measurements [NOAA, 1976]. No H $\alpha$  solar flare was detected at this time, however a large x-ray flare and a solar electron event consistent with this onset time were detected by both Helios 1 and Helios 2 [J. Trainor and A. Richter, personal communication]. The type III radio emission associated with this event was first detected by Helios 2 at about 0850 UT. The corresponding radio intensities detected by Helios 2, Hawkeye 1 and IMP 8 are shown in Figure 2. At the time of this event Helios 2 was east of the earth-sun line, at an earth-sun-probe angle of  $1.38^\circ$  and a heliocentric radial distance of 0.56 A. U., and Helios 1 was west of the earth-sun line, at an earth-sun-probe angle of  $28.8^\circ$  and a heliocentric radial distance of 0.34 A. U. The positions of Helios 1 and 2 projected onto the ecliptic plane are shown in Figure 3. The type III burst was not detected by Helios 1, probably because of the unfavorable viewing geometry for detecting the burst and the lower sensitivity of the Helios 1 instrument at high frequencies [see Gurnett and Anderson, 1977].

The direction of arrival measurements obtained for this event are summarized in Table 1. The time intervals used to obtain the parameters given in Table 1 were selected on the basis of a sliding average analysis and only those intervals which give a consistent direction of arrival for several successive contiguous intervals were used in computing the average directions of arrival. Reliable fits were obtained for three frequencies, 500, 178 and 100 kHz, from IMP 8, for two frequencies, 178 kHz and 100 kHz, from Helios 2 and for one frequency, 178 kHz, from Hawkeye 1. Although Table 1 shows results from Hawkeye 1 for 100 kHz, the standard deviation and fluctuations in the direction of arrival for this frequency are so large that this measurements was not used in the subsequent analysis. For all frequencies below 100 kHz the intensities and modulation factors were too small to give a reliable fit.

The directions of arrival projected onto the ecliptic plane are shown in Figure 3 for each frequency analyzed. The source positions at 100 and 178 kHz are indicated by the corresponding intersections of the directions of arrival from IMP 8 and Helios 2 for these frequencies. The crosshatched regions give the uncertainty in the source positions as determined from the estimated errors in  $\alpha_1$  and  $\alpha_2$  (see Table 1). Both the IMP 8 and Helios direction finding measurements clearly show a systematic eastward shift in the directions of arrival with decreasing frequency and increasing radial distance from the sun, characteristic of the typical Archimedean spiral trajectory of a type III burst. The best fit Archimedean spiral through the source positions

is shown in Figure 3. The equation used for the Archimedean spiral is

$$\varphi = \varphi_0 - \left(\frac{\Omega}{V_{SW}}\right)r ,$$

where  $\varphi$  and  $r$  are the heliographic longitude and radial distance,  $V_{SW}$  is the solar wind velocity, and  $\Omega$  is the rotational velocity of the sun. The solar wind velocity is assumed to be  $600 \text{ km sec}^{-1}$ . As will be discussed in the next section, this solar wind velocity is an approximate average value based on direct measurements by Helios 2 and IMP 8, with an appropriate delay to provide measurements in the source region. The trajectory of the type III burst in Figure 3 shows that the particles which produced the radio emission were emitted slightly east of the central meridian.

The position of the type III burst position out of the ecliptic plane, as determined by Hawkeye 1, is shown in the meridian plane projection of Figure 4. Unfortunately, accurate source positions in the meridian plane can only be obtained at one frequency, 178 kHz, for this event. Nevertheless, this measurement is important because it shows that the type III burst trajectory is very close to the ecliptic plane.

From the modulation factors given in Table 1 it is also possible to estimate the apparent size of the source. As can be easily shown the modulation factor is sensitive to the angular width of the source projected in the plane of rotation of the antenna. The modulation factor is the largest for a point source and decreases monotonically with increasing source size. The modulation factor is also affected

by the angular position of the source with respect to the spin plane of the antenna. Since the detailed shape of the source cannot be determined from this type of analysis some assumption must be made concerning the form of the source intensity distribution. For this analysis we have assumed that the source consists of a uniformly illuminated circular disk normal to the direction to the sun and centered on the source position determined from the triangulation measurements. Because of the geometric complexities the best fit source size must be determined by a computer fitting procedure which gives the best agreement with the measured modulation factors. For 178 and 500 kHz, which are the only frequencies analyzed, the half-angles of the source regions as viewed from the earth are  $36.5^\circ$  and  $10.5^\circ$ . It is evident that the source region of the type III radio emission at these frequencies is quite large. These source sizes are probably larger than the true size of the radiating region because of scattering in the interplanetary medium.

## IV. COMPARISON WITH THE SOLAR WIND DENSITY

Since the trajectory of the radio burst has been determined without reference to any specific model for the emission frequency these results can now be compared with the in situ plasma density measurements to determine the relationship of the emission frequency to the local electron plasma frequency. Fortunately the trajectory of the type III burst passed very close to the ecliptic plane, since this is the only region in which plasma density measurements are available. For this event plasma densities can be obtained over a wide range of heliocentric radial distances. Densities are available from IMP 7 and 8 at 1.0 A. U., from Helios 2 at about 0.55 A. U. and from Helios 1 at about 0.32 A. U. As shown in Figure 3 the trajectory of the type III burst passed eastward of all of these spacecraft. Therefore it is not possible to determine the plasma densities in the source region at the time of the burst. Instead the comparisons must be made a few days later, after the appropriate time delays for the solar rotation to bring the magnetic field line through the source region into coincidence with the spacecraft positions. The geometric considerations required to determine these time delays are illustrated in Figure 5, which shows the trajectories of IMP 7 and 8, Helios 2 and Helios 1 in a coordinate system fixed to the sun. The appropriate time delays are approximately 3.9 days for IMP 7 and 8, 2.6 days for Helios 2 and 8 days for Helios 1.

Since the large scale rotational structure of the solar wind has been found to be quite consistent and repeatable for several solar rotations during solar minimum conditions, it is believed that any temporal changes which may have occurred in the plasma density during this few day period should be small. Fortunately, the shortest delay is for Helios 2 which passes the closest to the observed source locations (compare Figures 3 and 5).

The solar wind plasma densities obtained from IMP 7 and 8, Helios 2, and Helios 1 are shown in Figure 6. Although the plasma instruments actually measure ion densities, the measurements shown are equivalent electron densities computed assuming the plasma is electrically neutral. The time scales in Figure 6 are adjusted so that measurements obtained at the same heliographic longitude are aligned vertically. The points A, B and C correspond to times when the spacecraft cross the best fit trajectory of the type III burst. Although large variations in the electron density are evident, particularly in the IMP 7 and 8 data, the density is relatively smooth and constant in the region near the type III burst trajectory. The density enhancement evident at all three radial distances (day 87 at Helios 1, days 83 and 84 at Helios, and days 85 and 86 at IMP 7 and 8) is evidently a co-rotating structure which has an Archimedean spiral structure similar to the type III burst, but displaced approximately  $20^\circ$  westward in longitude. The corresponding solar wind velocity variations, illustrated in Figure 7, show that this density compression precedes the onset of a high-speed stream, following the well known pattern discussed by Hundhausen [1973]. The steepening

of solar wind velocity profile and the increase in the fractional amplitude of the density perturbation in the compression region with increasing radial distance from the sun is clearly evident. The good qualitative agreement between the observed solar wind velocity and density profiles and the variations expected for a nearly stationary co-rotating solar wind structure give us added confidence that valid comparisons can be made with the local plasma densities several days after the event.

When the electron plasma frequencies obtained from these plasma densities are compared with the observed emission frequencies consideration must be given to the uncertainties in the position of the source and the apparent size of the source. Although points A, B and C in Figure 6 represent the best estimate of the type III trajectory, based on the Archimedean spiral fit, these intersections are somewhat uncertain because of our lack of knowledge of the exact structure of the solar wind magnetic field. Point C probably has the largest error because it represents an extrapolation by several tenths of an A. U. into a region where the Archimedean spiral angle is quite sensitive to the solar wind velocity. Note from Figure 7 that the solar wind velocity,  $V_{SW} = 600 \text{ km sec}^{-1}$ , used in the Archimedean spiral fit is in close agreement with the velocities measured by Helios 2 and IMP 7 and 8. Point B on the other hand is probably very accurate since it is determined by an interpolation between measured source positions less than 0.2 A. U. apart. Point A is also considered to be reasonably accurate since the Archimedean spiral model for the magnetic field is less subject to errors

close to the sun. Also, in the region close to the sun the direction finding measurements (500 kHz in Figure 3) show good qualitative agreement with the best fit Archimedean spiral, even though exact source positions cannot be determined by triangulation.

Because of the large apparent source size a choice must be made concerning the size of the region over which the electron densities are to be compared. Although the IMP 8 and Hawkeye 1 spin modulation measurements indicate that the source subtends a half-angle of about  $40^\circ$ , as viewed from the sun, this source size is almost certainly determined by scattering and is too large. This viewpoint is supported by the Helios-2 measurements at 178 kHz which still have a sizeable spin modulation ( $m = 0.44$ , which corresponds to a half-angle of about  $46^\circ$  for a uniformly illuminated disk) even though the spacecraft is only  $18^\circ$  in heliographic longitude from the center of the source. These results suggest that the angular size of the source is on the order of 10 to  $15^\circ$  half-angle, as viewed from the sun, or possibly even smaller. On the basis of these estimates of the source size we have averaged the electron density measurements over a region of  $\pm 10^\circ$  heliographic longitude on either side of the centroid of the source as determined by the points A, B and C in Figure 6.

The average electron plasma frequencies within the  $\pm 10^\circ$  regions centered on points A, B and C are shown in Figure 8, plotted as a function of heliocentric radial distance. The standard deviation of the plasma frequency in each region is also shown by the error bars in Figure 8, to indicate the range of variability of the plasma frequency

in the assumed source region. The electron plasma frequency is also considered to be uncertain by about  $\pm 15\%$  because of instrumental limitations in the absolute density determination [W. Feldman, personal communication]. Also shown in Figure 8 are the observed type III emission frequencies and their corresponding heliocentric radial distances, as determined from the triangulation measurements in Figure 3. The error limits on the emission frequencies and radial distances, indicated by the crosshatched regions, are determined by the filter bandwidths ( $\pm 7.5\%$ ) and the uncertainties in the triangulation measurements.

The systematic decrease in the solar wind plasma frequency and the type III emission frequency with increasing heliocentric radial distance is clearly evident in Figure 8. The electron plasma frequencies are seen to be in good agreement with the expected  $1/R$  variation with radial distance, as indicated by the solid line. The emission frequencies are in all cases substantially above the local electron plasma frequency, too far removed to be consistent with generation of the radiation at  $f_p^-$ . For comparison the second harmonic of the electron plasma frequency,  $2f_p^-$ , is shown by the dashed line in Figure 8, based on the  $1/R$  curve through the average plasma frequencies. The observed emission frequencies are seen to be in reasonably good agreement with the second harmonic,  $2f_p^-$ , much better than for the fundamental,  $f_p^-$ .

## V. SUMMARY AND DISCUSSION

By using long baseline stereoscopic direction finding measurements from the IMP 8, Hawkeye 1 and Helios 2 spacecraft the three-dimensional trajectory of a type-III solar radio burst has been determined and analyzed. In contrast to previous direction finding analyses of type-III radio bursts the trajectory in this case was obtained completely independent of any modeling assumptions regarding the radial dependence of the emission frequency. Comparisons of the observed emission frequencies with the plasma densities measured along the trajectory were used to determine whether the radiation is generated at the fundamental,  $f_p^-$ , or second harmonic,  $2f_p^-$ , of the local electron plasma frequency. For the event analyzed the results show that the radio emission is generated near the second harmonic,  $2f_p^-$ , and not at the fundamental.

In considering possible uncertainties in our result several factors must be considered. The primary uncertainties in the analysis are concerned with (1) the constancy of the solar wind density distribution from the time the event occurred until the time that the density measurements were obtained, (2) the size of the source and (3) the plasma densities out of the ecliptic plane. The temporal stability of the rotating solar wind structure during the period of interest is supported by the close agreement between the solar wind velocity and density variations observed by IMP 7 and 8 near the earth and by Helios 1 and

2 closer to the sun and by the fact that the solar wind sector structure is relatively steady and repeatable for several solar rotations during solar minimum. The uncertainty regarding the source size arises because of the necessity for comparing a large scale average property, the emission frequency, with a series of local measurements. Because of the presently unknown role of scattering in the interplanetary medium the actual source size is not easily related to the apparent source size given by the modulation factor measurements. Since the actual source size is not well known, except for an upper limit, the size of the region over which the electron density must be averaged to compute the "average" electron plasma frequency is not accurately known. Fortunately, the spatial variations in the plasma frequency are not so large that the basic conclusion is affected by the assumed size of the source region. Even if the source size is increased by a factor of two or more, the electron plasma frequencies detected by Helios 1 and 2 are not changed sufficiently to be consistent with generation of the radiation at the fundamental. Another limitation is that in situ plasma density measurements are only available near the ecliptic plane. It is, of course, possible that the plasma density is unexpectedly large in the region away from the ecliptic plane, in which case the radiation could be generated at the fundamental and still be consistent with our measurements. Since the centroid of the source is located very close to the ecliptic plane (see Figure 4) this hypothesis is not considered very likely since it would require that the average plasma density increase symmetrically, by at least a factor of 4, within a few degrees on either side of the ecliptic plane. Considering

the observed range of longitudinal variations such large latitudinal variations of the plasma density away from the ecliptic plane seem quite unlikely.

The conclusion of this investigation, that the low-frequency type-III radio emission is generated at  $2f_p^-$ , is consistent with and confirms the earlier results of Fainberg et al. [1972], Haddock and Alvarez [1973], Fainberg and Stone [1974], Alvarez et al. [1975], and Kaiser [1975].

The main advantage of this study is that the relationship is determined directly by comparisons with in situ measurements rather than relying on an assumed model for the radial dependence of the emission frequency and/or average statistical properties of the solar wind.

## ACKNOWLEDGMENTS

The authors express their thanks to Dr. William Feldman from the Los Alamos Scientific Laboratory for providing the IMP 7 and 8 plasma densities and velocities used in this study.

The research at the University of Iowa was supported in part by NASA under Contracts NAS5-11431, NAS1-13129 and NAS5-11279 and Grant NGL-16-001-043 and by the Office of Naval Research under Contract N00014-76-C-0016.

## REFERENCES

- Alvarez, H., F. T. Haddock, and R. P. Lin, Evidence for electron excitation of type III radio burst emission, Solar Physics, 26, 468, 1972.
- Alvarez, H., R. P. Lin, and S. J. Bame, Fast solar electrons, interplanetary plasma and km-wave type-III radio bursts observed from the IMP-6 spacecraft, Solar Physics, 44, 485, 1975.
- Alvarez, H., F. T. Haddock, W. H. Potter, J. Fainberg, R. J. Fitzenreiter and R. R. Weber, Out-of-ecliptic trajectories of low frequency type III bursts, Solar Physics (in press), 1976.
- Asbridge, J. R., S. J. Bame, W. C. Feldman, and M. D. Montgomery, Helium and hydrogen velocity differences in the Solar Wind, J. Geophys. Res., 81, 2719, 1976.
- Baumback, M. M., W. S. Kurth, and D. A. Gurnett, Direction finding measurements of type III radio bursts out of the ecliptic plane, Solar Physics, 48, 361, 1976.
- Fainberg, J., L. G. Evans, and R. G. Stone, Radio tracking of solar energetic particles through interplanetary space, Science, 178, 743, 1972.

Fainberg, J. and R. G. Stone, Satellite observations of type III solar radio bursts at low frequencies, Space Sci. Rev., 16, 145, 1974.

Frank, L. A. and D. A. Gurnett, Direct observations of low-energy solar electrons associated with a type III solar radio burst, Solar Physics, 27, 446, 1972.

Ginzburg, V. L. and V. V. Zheleznyakov, On the possible mechanism of sporadic solar radio emission (radiation in an isotropic plasma), Sov. Astron. AJ2, 653, 1958.

Gurnett, D. A. and R. R. Anderson, Electron plasma oscillations associated with type III radio bursts, Science, 194, 1159, 1976.

Gurnett, D. A. and R. R. Anderson, Plasma wave electric fields in the solar wind: initial results from Helios-1, J. Geophys. Res. 82, 632, 1977.

Haddock, F. T. and H. Alvarez, The prevalence of second harmonic radiation in type III bursts observed at kilometric wavelengths, Solar Physics, 29, 183, 1973.

Hundhausen, A. J., Nonlinear model of high-speed solar wind streams, J. Geophys. Res., 78, 1528, 1973.

Kaiser, M. L., The solar elongation distribution of low frequency radio bursts, Solar Physics, 45, 181, 1975.

Kurth, W. S., M. M. Baumbach, and D. A. Gurnett, Direction-finding measurements of auroral kilometric radiation, J. Geophys. Res., 80, 2764, 1975.

Lin, R. P., The emission and propagation of  $\sim 40$  keV solar flare electrons, Solar Physics, 12, 266, 1970.

Lin, R. P., L. G. Evans, and J. Fainberg, Simultaneous observations of fast solar electrons and type III radio burst emission near 1 AU, Astrophys. Lett., 14, 191, 1973.

NOAA, Solar-Geophysical Data, 385 Part II, 22, September 1976.

Papadopoulos, K., M. L. Goldstein and R. A. Smith, Stabilization of electron streams in type III solar radio bursts, Astrophys. J., 190, 175, 1974.

Parker, E. N., Dynamics of the interplanetary gas and magnetic fields, Astrophys. J., 128, 664, 1958.

Schwenn, R., H. Rosenbauer, and H. Miggenrieder, Das plasmaexperiment auf Helios (E1), Raumfahrtforschung, 19(5), 226, 1975.

Smith, D. F., Type III radio bursts and their interpretation, Space Sci. Rev., 16, 91, 1974.

Sturrock, P. A., Spectral characteristics of type III solar radio bursts, Nature, 192, 58, 1961.

Tidman, D. A., T. J. Birmingham, and H. M. Stainer, Line splitting of plasma radiation and solar radio outbursts, Astrophys. J., 146, 207, 1966.

Wild, J. P., Observations of the spectrum of high-intensity solar radiation at metre wavelengths (III. Isolated bursts), Aust. J. Sci. Res., A3, 541, 1950.

Wild, J. P., M. D. Murray, and W. C. Rowe, Harmonics in the spectra of solar radio disturbances, Aust. J. Phys., 7, 439, 1954.

Table 1

Frequency	Helios 2		IMP 8		Hawkeye 1	
	$\alpha_2$	m	$\alpha_1$	m	$\beta_1$	m
500 kHz	--	--	$3.9^\circ \pm 1.1^\circ$	0.985	--	--
178 kHz	$42.0^\circ \pm 0.4^\circ$	0.444	$17.4^\circ \pm 1.2^\circ$	0.809	$4.1^\circ \pm 0.6^\circ$	0.448
100 kHz	$78.0^\circ \pm 4.1^\circ$	0.047	$35.4^\circ \pm 0.6^\circ$	0.521	$24.7^\circ \pm 9.4^\circ$	0.130

## FIGURE CAPTIONS

- Figure 1      The geometry used for the three-dimensional stereoscopic direction finding with IMP 8, Hawkeye 1 and Helios. The spin modulation gives the direction of arrival projected onto a plane perpendicular to the spacecraft spin axis. IMP 8 and Helios have their spin axes perpendicular to the ecliptic plane which gives the angles  $\alpha_1$  and  $\alpha_2$ , thereby determining the source position projected onto the ecliptic plane. Hawkeye 1 has its spin axis nearly parallel to the ecliptic plane, which gives the angle  $\beta_1$ , thereby determining the source position out of the ecliptic plane.
- Figure 2      The electric field intensities detected by IMP 8, Hawkeye 1 and Helios 2 for the type III radio burst on day 83, March 23, 1976. The larger intensities detected by IMP 8 are due to the longer antenna length, 121.8 meters tip-to-tip for the IMP 8 plasma wave experiment, compared to 42.45 meters for Hawkeye 1 and 32.0 meters for Helios 2.
- Figure 3      The ecliptic plane projection of the source positions determined by triangulation from IMP 8 and Helios 2. The uncertainty in the centroid of the source position is indicated by the crosshatched regions at the intersections

of the directions of arrival. The best fit trajectory is an Archimedean spiral through the observed source positions. The parameters of the Archimedean spiral have been selected to represent the expected configuration of the solar wind magnetic field for a solar wind velocity of 600 km/sec.

Figure 4      The observed source position of the type III burst in the meridian plane. Unfortunately, reliable direction finding measurements can only be obtained for one frequency, 178 kHz, from Hawkeye 1 during this event. This one measurement does however show that the trajectory of the type III was very close to the ecliptic plane.

Figure 5      The trajectories of IMP 7 and 8, Helios 2 and Helios 1 in a coordinate system fixed to the sun. The spacecraft intersect the best fit trajectory of the type-III burst at the points marked A, B and C. Point B represents the best position for comparisons with the local plasma frequency since this intersection is the closest to the observed source positions (compare with Figure 3) and occurs at the shortest time (2.6 days) after the event.

- Figure 6     The electron densities observed by IMP 7 and 8, Helios 2 and Helios 1 for the several day period after the type III event on day 83. The intersections with the best fit trajectory occur at points A, B and C, as determined from Figure 5.
- Figure 7     The solar wind velocity observed by IMP 7 and 8, Helios 2 and Helios 1 for the several day period after the type III event on day 83. Note that the velocities at B and C are in close agreement with the assumed velocity of  $600 \text{ km sec}^{-1}$  used for the best fit Archimedean spiral in Figure 3. The velocity at A is lower, however the shape of the best fit spiral is less sensitive to the velocity in the region close to the sun.
- Figure 8     A comparison of the observed emission frequencies of the type III burst and the measured electron plasma frequencies as a function of radial distance from the sun. Since the angular size of the source is rather large, as viewed from the earth, the electron plasma frequencies have been averaged over a longitude range of  $\pm 10^\circ$  centered on the points A, B and C in Figure 6. The error bars give the standard deviation of the electron plasma frequency over this interval.

A-G76-924

31

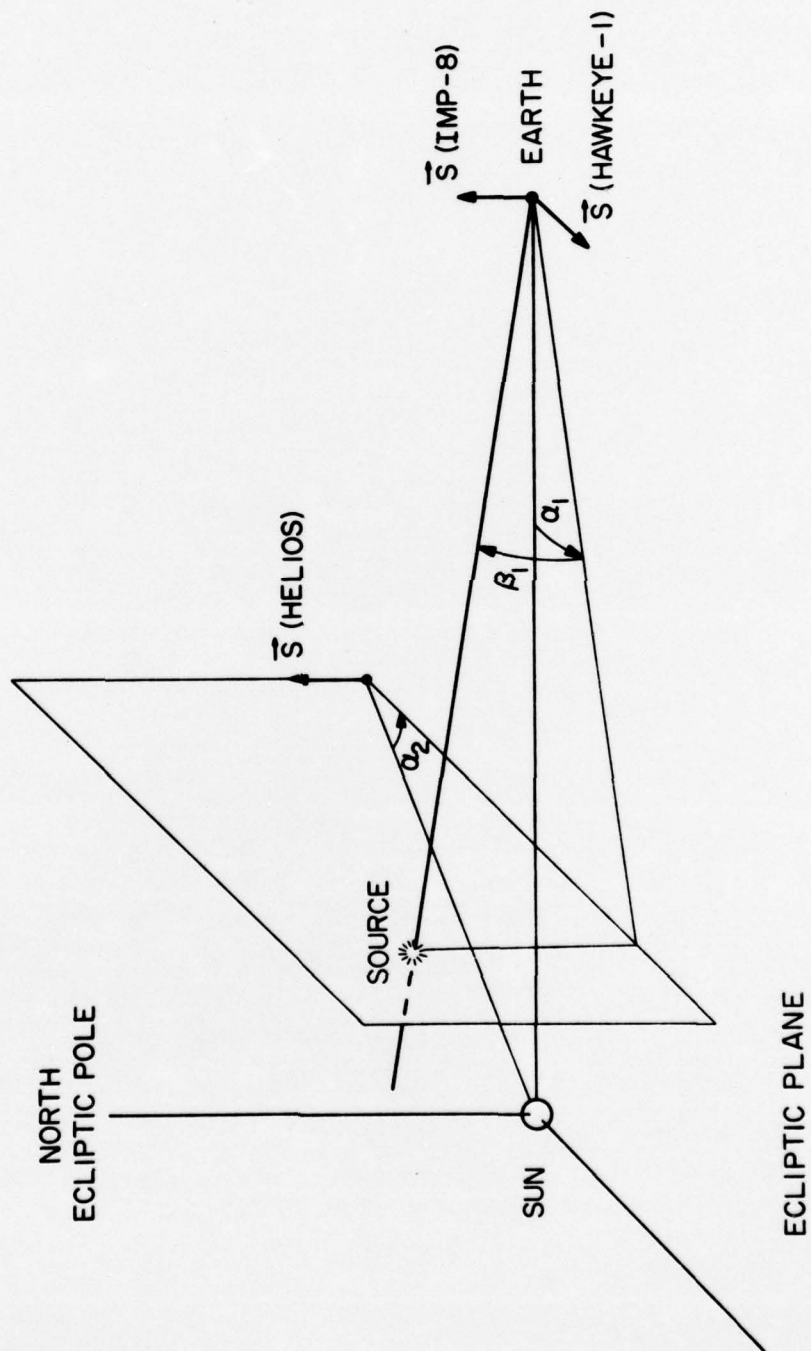


Figure 1

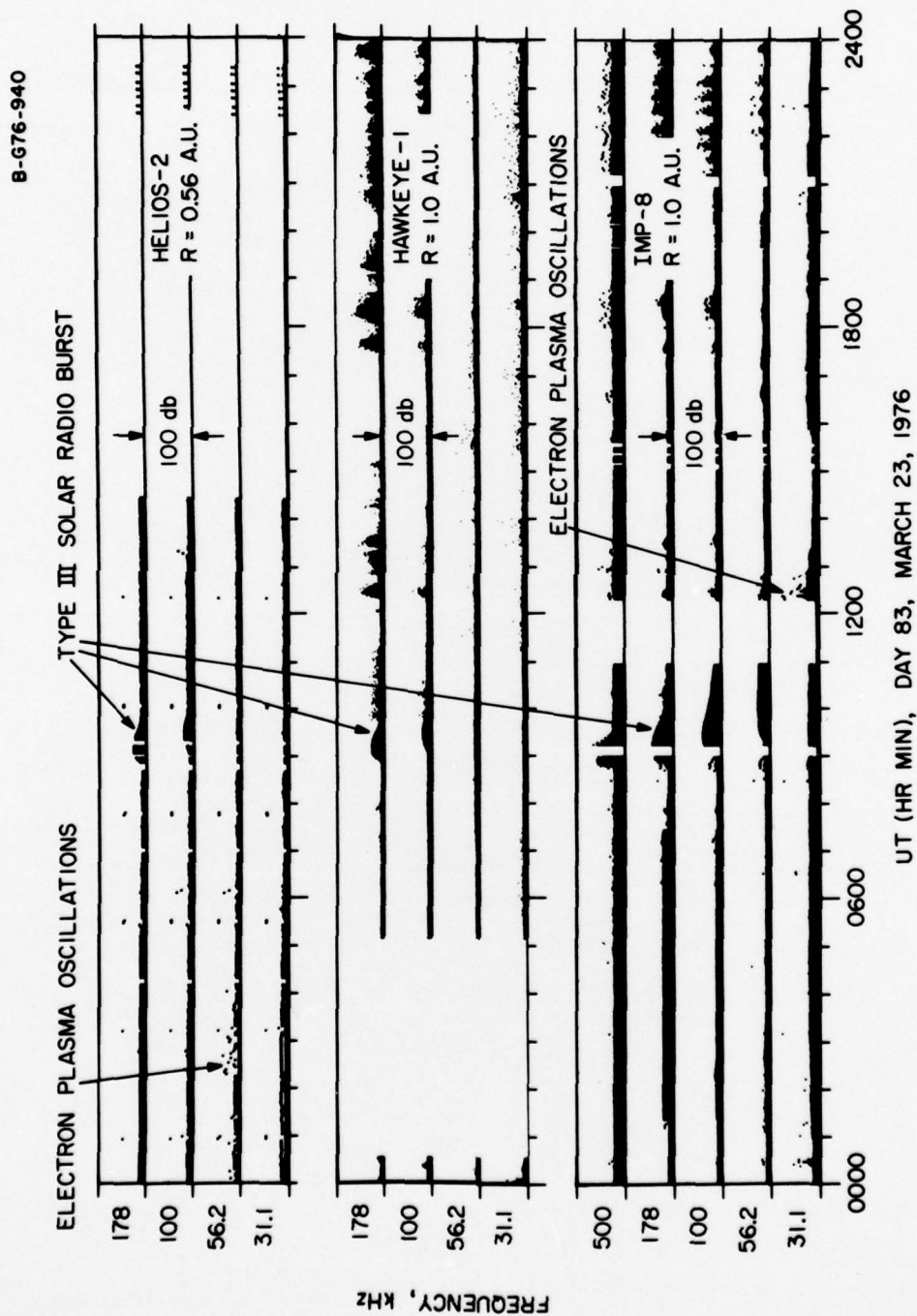


Figure 2

C-676-928-1

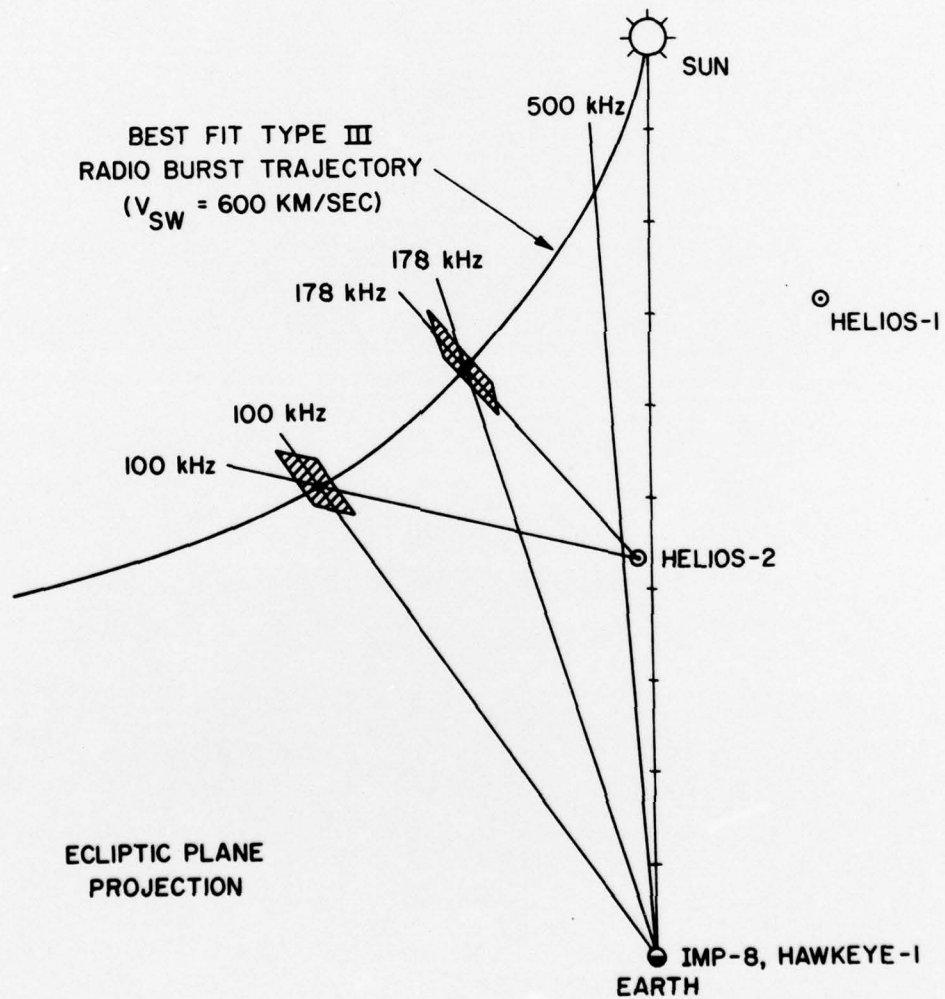


Figure 3

B-G77-91

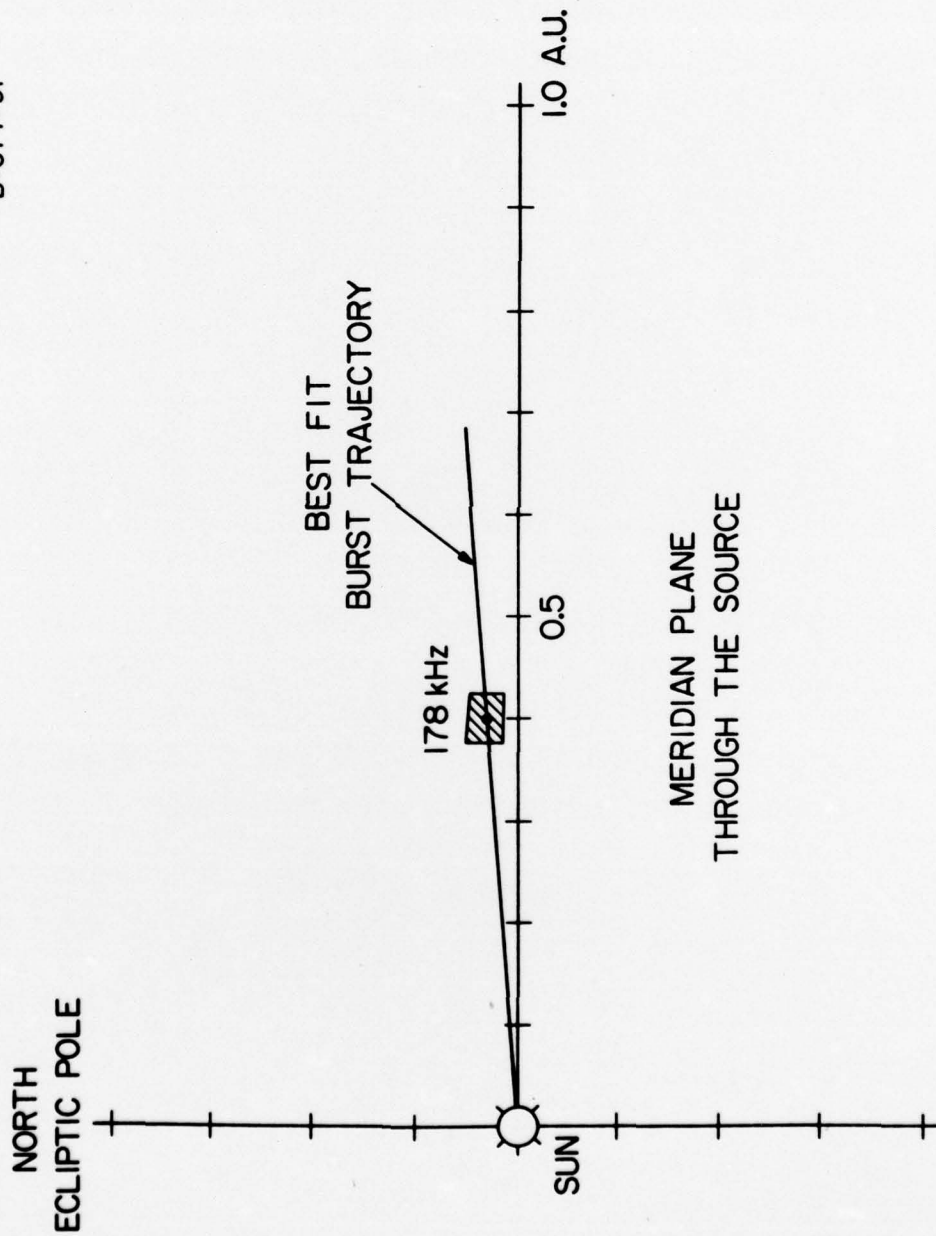


Figure 4

C-G76-927-1

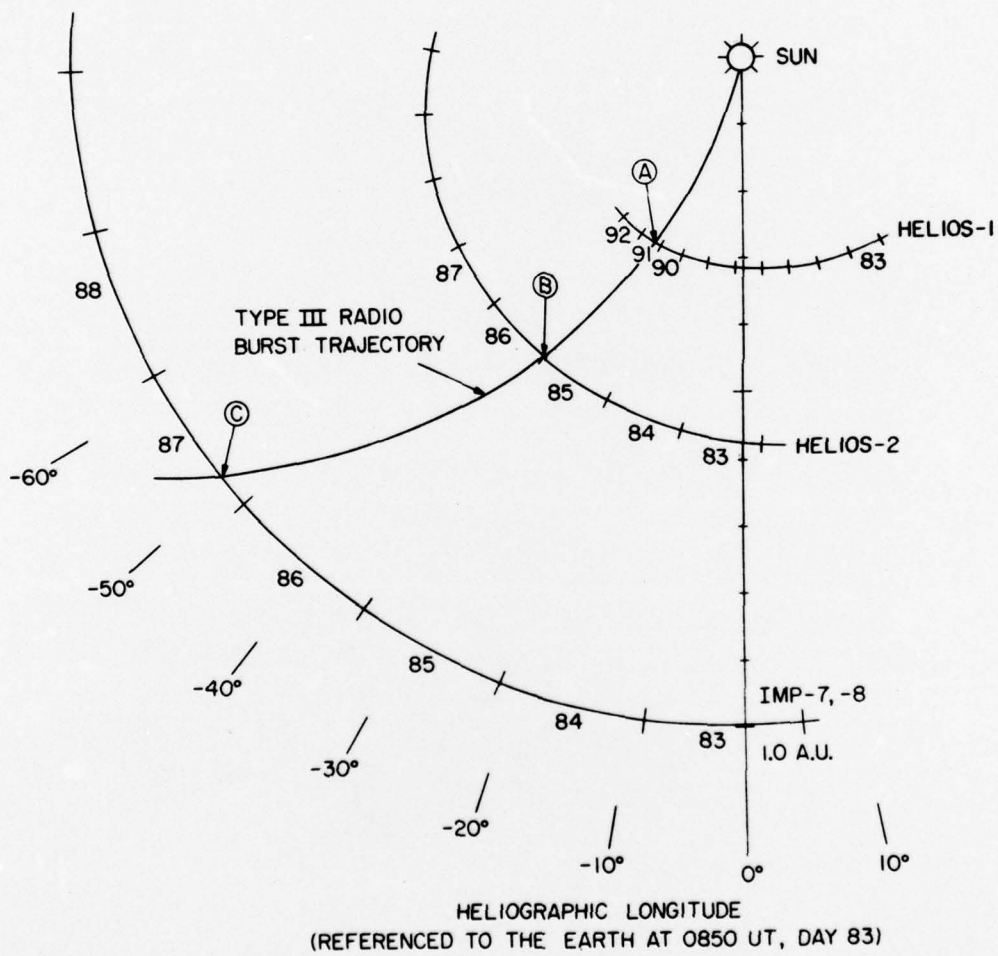


Figure 5

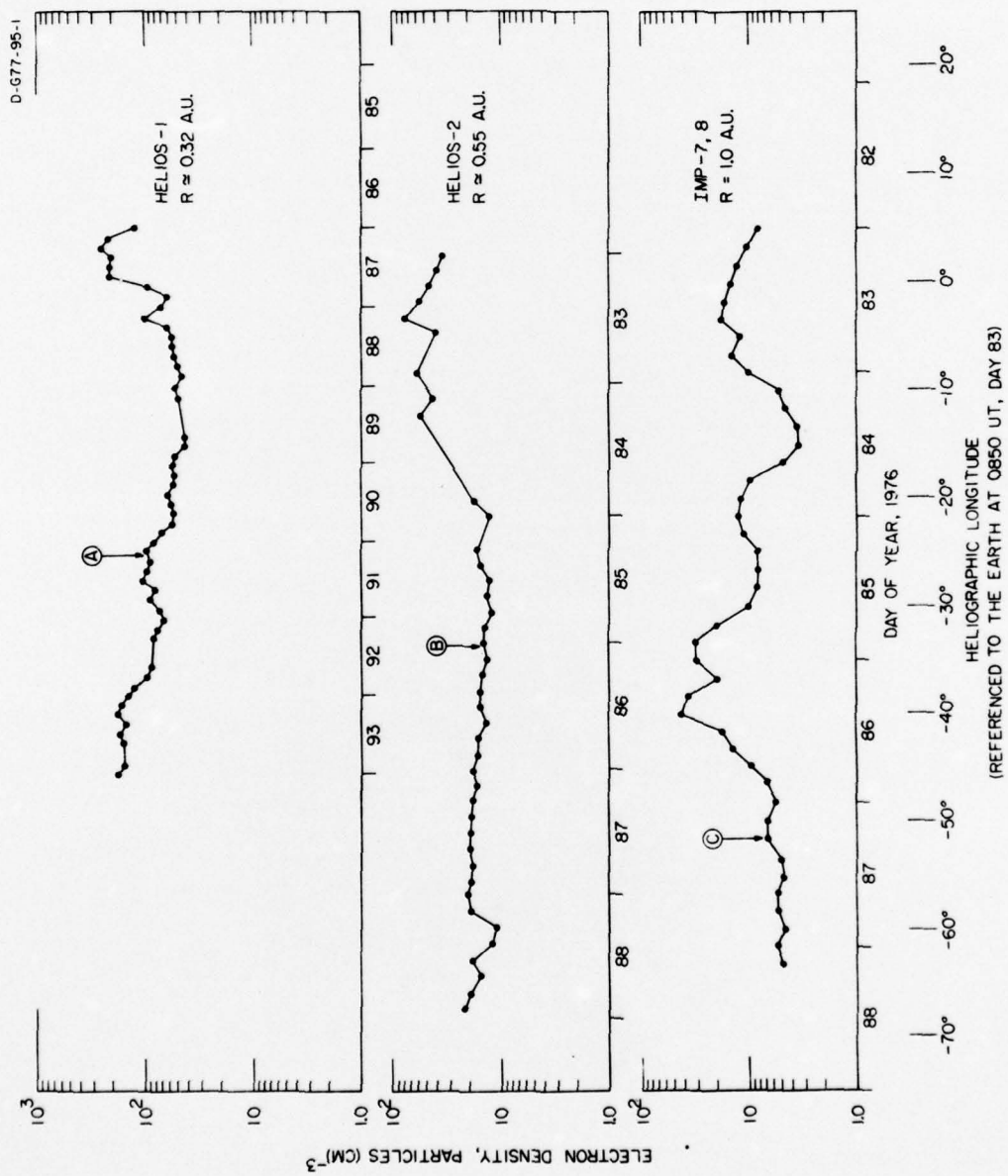


Figure 6

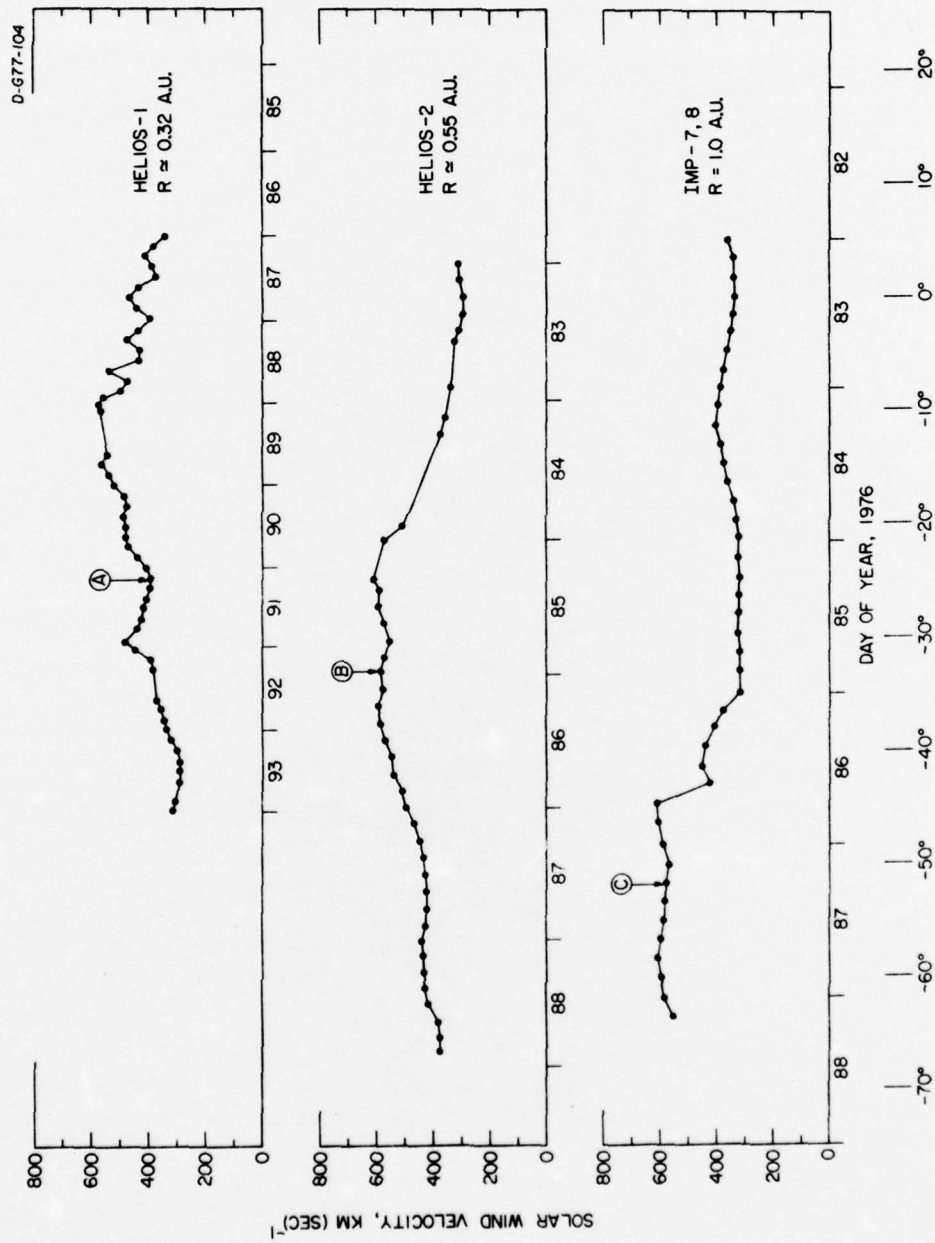


Figure 7

A-G77-94

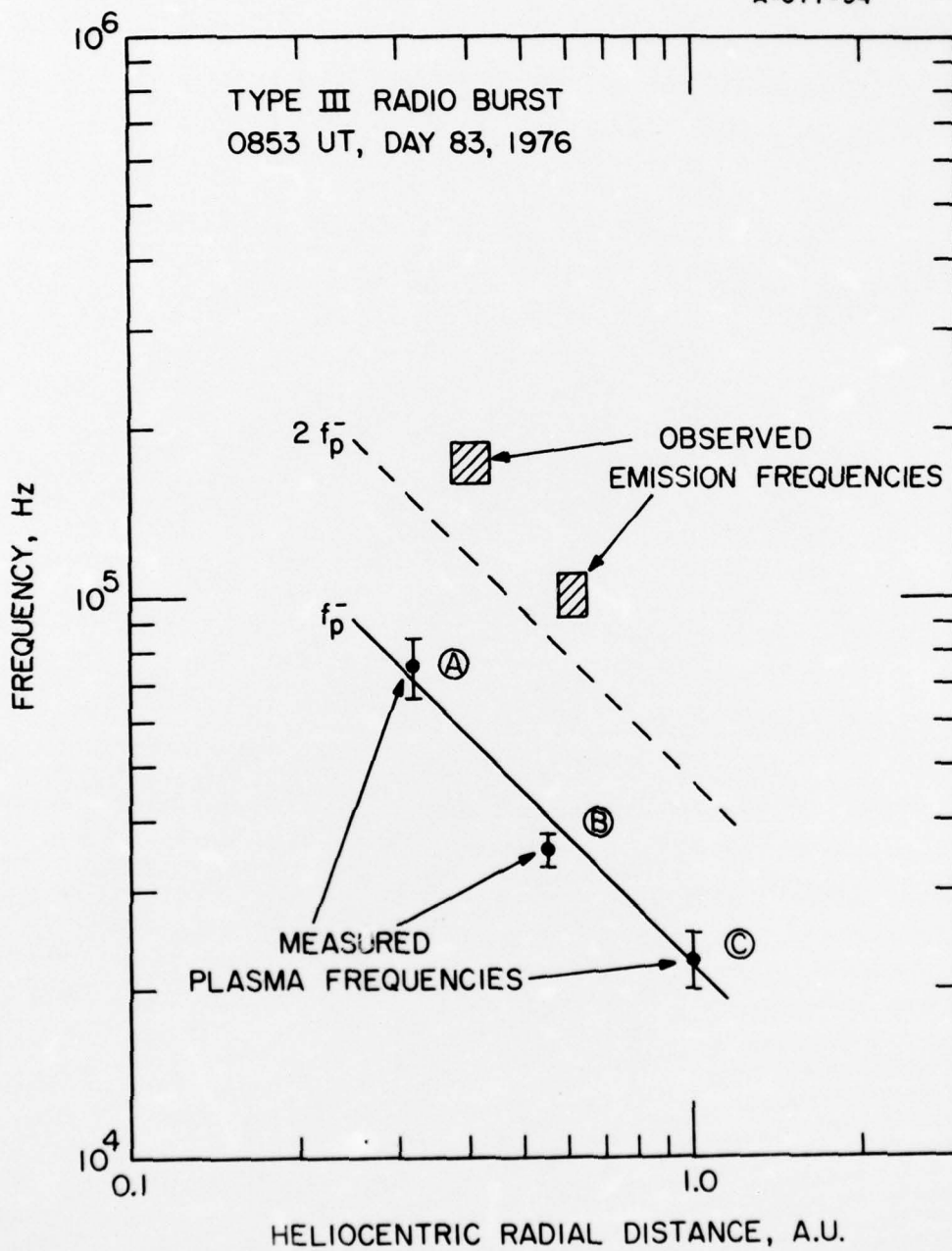


Figure 8